THE JOURNAL OF BIOLOGICAL CHEMISTRY VOL. 289, NO. 6, pp. 3602–3612, February 7, 2014

O-Linked β-*N*-Acetylglucosamine (*O*-GlcNAc) Site Thr-87 Regulates Synapsin I Localization to Synapses and Size of the Reserve Pool of Synaptic Vesicles*[S]

Received for publication, October 31, 2013 Published, JBC Papers in Press, November 26, 2013, DOI 10.1074/jbc.M113.512814

Yuliya Skorobogatko[‡], Ashly Landicho[‡], Robert J. Chalkley[§], Andrew V. Kossenkov[¶], Gianluca Gallo[‖], and Keith Vosseller[‡1]

From the [‡]Department of Biochemistry, Drexel University College of Medicine, Philadelphia, Pennsylvania 19102, the [§]University of California, San Francisco, California 94158, the [¶]Bioinformatics Facility, The Wistar Institute, Philadelphia, Pennsylvania 19104, and the [‖]Shriners Hospitals Pediatric Research Center, Department of Anatomy and Cell Biology, Temple University, Philadelphia, Pennsylvania 19140

Background: Synapsin I regulates synaptic plasticity and is modified by *O*-GlcNAc.
Results: Mutation of *O*-GlcNAc site Thr-87 to alanine increases both localization of synapsin I to synapses and the reserve pool of synaptic vesicles.
Conclusion: *O*-GlcNAcylation of Thr-87 may regulate synapsin I localization and function.
Significance: *O*-GlcNAcylation of synapsin I may modulate synaptic plasticity.

_O_-GlcNAc is a carbohydrate modification found on cytosolic and nuclear proteins. Our previous findings implicated _O_-GlcNAc in hippocampal presynaptic plasticity. An important mechanism in presynaptic plasticity is the establishment of the reserve pool of synaptic vesicles (RPSV). Dynamic association of synapsin I with synaptic vesicles (SVs) regulates the size and release of RPSV. Disruption of synapsin I function results in reduced size of the RPSV, increased synaptic depression, memory deficits, and epilepsy. Here, we investigate whether _O_-GlcNAc directly regulates synapsin I function in presynaptic plasticity. We found that synapsin I is modified by _O_-GlcNAc during hippocampal synaptogenesis in the rat. We identified three novel _O_-GlcNAc sites on synapsin I, two of which are known Ca^{2+}/calmodulin-dependent protein kinase II phosphorylation sites. All _O_-GlcNAc sites mapped within the regulatory regions on synapsin I. Expression of synapsin I where a single _O_-GlcNAc site Thr-87 was mutated to alanine in primary hippocampal neurons dramatically increased localization of synapsin I to synapses, increased density of SV clusters along axons, and the size of the RPSV, suggesting that _O_-GlcNAcylation of synapsin I at Thr-87 may be a mechanism to modulate presynaptic plasticity. Thr-87 is located within an amphipathic lipid-packing sensor (ALPS) motif, which participates in targeting of synapsin I to synapses by contributing to the binding of synapsin I to SVs. We discuss the possibility that _O_-GlcNAcylation of Thr-87 interferes with folding of the ALPS motif, providing a means for regulating the association of synapsin I with SVs as a mechanism contributing to synapsin I localization and RPSV generation._

O-Linked β-*N*-acetylglucosamine (*O*-GlcNAc)[2] is a regulatory carbohydrate modification of intracellular proteins. *O*-GlcNAc and enzymes executing its turnover (*O*-GlcNAc transferase and *O*-GlcNAcase) are enriched in brain (1). Brain *O*-GlcNAcylation is modulated during development and neurotransmission, suggesting potential regulatory roles of *O*-GlcNAc in these processes (2–7). Current knowledge is still insufficient to draw a clear picture for the physiological function of *O*-GlcNAc signaling in the brain, but there is growing evidence that *O*-GlcNAc may regulate synaptic plasticity, a property of neurons to modulate the strength of communication between synapses that is indispensible for learning and memory (6, 8).

We previously demonstrated that elevation of *O*-GlcNAc in mouse brain facilitates hippocampal CA1 long term potentiation (an electrophysiological readout of a form of synaptic plasticity) at least in part through a presynaptic mechanism (8). Additionally, ours and others proteomic studies identified uniquely extensive *O*-GlcNAcylation of presynaptic proteins involved in organization and mobilization of synaptic vesicles (SVs), including bassoon, piccolo, and synapsins I and II (9–11). Although bassoon and piccolo serve as scaffolds for assembly of the presynaptic active zone, synapsins are regulatory proteins involved in synaptic plasticity. Synapsins dynamically bind SVs and are required during synaptogenesis and in mature neurons for the establishment and regulation of the reserve pool of SVs (RPSV) (12). RPSV is a group of SVs that is located distal from the synaptic cleft and is released only during high frequency stimulation (HFS), as opposed to the readily releasable pool of

* This work was supported, in whole or in part, by National Institutes of Health Grant R21AG033226-02 from NIA (to K. V.) and Grant 8P41GM103481 from NIGMS (to R. J. C.). This work was also supported by Mars Audrey Meyer Fellowship in Aging Research at Drexel University College of Medicine.
[S] This article contains supplemental Fig. 1 and Table 1.
[1] To whom correspondence should be addressed: Dept. of Biochemistry, Drexel University College of Medicine, 245 N. 15th St., NCB, Rm. 10-112, Philadelphia, PA 19102. Tel.: 215-762-8788; Fax: 215-762-4452; E-mail: Keith.Vosseller@drexelmed.edu.

[2] The abbreviations used are: *O*-GlcNAc, *O*-linked β-*N*-acetylglucosamine; ALPS, amphipathic lipid-packing sensor motif; HFS, high frequency stimulation; SV, synaptic vesicle; RPSV, reserve pool of SVs; RRPSV, readily releasable pool of SV; TF, targeting factor; WB, Western blotting; CaMKII, Ca^{2+}/calmodulin-dependent protein kinase II; EGFP, enhanced GFP; Ab, antibody; ncOGT, nucleocytoplasmic OGT; ANCOVA, analysis of covariance; mRFP, monomeric red fluorescent protein; AFU, arbitrary fluorescent unit.

SVs (RRPSV), which is located in close proximity to the synaptic cleft and is released in response to low frequency stimulation (13). Regulation of RPSV formation by synapsins contributes to presynaptic plasticity and is important for memory formation. For example, in synapsin I- and II-null mice, synapses are still formed but are not fully functional because the RPSV is dramatically decreased. The mice demonstrate defects in synaptic plasticity (more pronounced synaptic depression), age-related cognitive decline, and epileptic seizures (14). Mutations in synapsin I have also been found in patients with epilepsy and autism spectrum disorders (15, 16). The following model of RPSV regulation by synapsins has been developed so far. During synaptogenesis, synapsins increasingly localize to synapses, tethering SVs to each other and possibly to an actin-based cytoskeleton. Thus, synapsins establish RPSV and prevent RPSV from being released during low frequency stimulation. During HFS, synapsins dissociate from SVs and disperse from synapses into the axonal shaft, allowing for the release of RPSV (17).

The synapsin protein family includes the products of three genes: synapsin I, II, and III. Among these family members, the role and regulation of synapsin I in presynaptic plasticity are best understood. Because of alternative splicing, two isoforms arise from the synapsin I gene, synapsin Ia and Ib, which contain different short C-terminal domains E and F, respectively. Phosphorylation of synapsin I by several kinases is important for its function in synaptic plasticity. Association of synapsin I with SVs is regulated by phosphorylation at PKA and CaMKII phosphorylation sites (18, 19); the speed of synapsin dispersion during HFS is regulated by phosphorylation at ERK and CaMKII phosphorylation sites (20); phosphorylation of synapsin by ERK affects the distribution of SVs between RPSV and RRPSV (21). All these phosphorylation sites (with the exception of the PKA phosphorylation site) are localized within regulatory domains B and D. These domains are relatively short and mostly unstructured regions that flank the large globular central domain C in synapsins. Domains B and D of synapsin I are also modified by *O*-GlcNAc, suggesting possible regulatory function for *O*-GlcNAcylation (22). The biological role of *O*-GlcNAc on synapsin I has not been previously addressed and is the focus of this study.

EXPERIMENTAL PROCEDURES

Purification of Synapsin I and Mass Spectrometry—C57BL/6 mice were sacrificed by cervical dislocation, and brains were removed. Alternatively, frozen bovine brain was purchased from Sierra for Medical Science, Whittier, CA. Synapsin I was purified from the brains by detergent extraction under nondenaturing conditions as described previously with some modifications (23). Elution from a hydroxyapatite column was performed with a 0–100% gradient of the following buffer: 250 mM $Na_nH_nPO_4$ (pH 7.4), 150 mM NaCl, 2 mM EDTA, 0.1 mM EGTA, 0.5 mM β-mercaptoethanol (24). Synapsin I, which eluted as a sharp peak, was collected and used for mass spectrometry directly or dialyzed into storage buffer (50 mM $Na_nH_nPO_4$ (pH 7.4), 60 mM NaCl, 2 mM EDTA, 0.1 mM EGTA, 0.5 mM β-mercaptoethanol, 10% glycerol) and stored at −80 °C. Trypsin digestion, nanospray ESI-LC-MS/MS/MS analysis by linear ion trap using collision-induced dissociation, LC MS/MS using electron transfer dissociation, and sequence data analyses were performed as described previously (25, 26). A custom fasta database containing bovine and mouse synapsin 1 proteins was created and searched with Xcalibur software in BioWorks. A potential variable modification of 203.08 daltons on serines/threonines was considered during searches to identify potentially *O*-GlcNAc-modified residues. Manual checking of Y and B ion series or in the case of electron transfer dissociation spectra, C and Z ion series, was determined to assign peptide sequence and *O*-GlcNAc modification sites.

TABLE 1
Generated *O*-GlcNAc site-specific mutants of synapsin I

Designation	Introduced amino acid substitutions
Syn1a or WT	Wild type
Syn1a_1–3	S55A, T56A, T87A
Syn1a_5–8	S516A, S518A, T521A, T524A
Syn1a_5–10	S516A, S518A, T521A, T524A, T562A, S576A
Syn1a_4–11	S516A, S518A, T521A, T524A, T562A, S576A, T615A, T616A
Syn1a_1–11	S55A, T56A, T87A, S516A, S518A, T521A, T524A, T562A, S576A, T615A, T616A
Syn1a_S62E,S67E	S62E, S67E
Syn1a_1–3_S62,67A	S55A, T56A, T87A, S62E, S67E
Syn1a_S55A	S55A
Syn1a_T56A	T56A
Syn1a_T87A or T87A	T87A

Synapsin Pulldown from Rat Brain Lysates—Rat pups (Holzman rat from Harlan Laboratories, Indianapolis, IN) of various ages where euthanized with CO_2 and decapitated. Hippocampi were dissected and then lysed based on the synapsin purification protocol (23). Lysates containing 4.5 mg of protein were processed to pull down synapsin I as described previously, but with batch absorption on CM-52 cellulose performed overnight (27). 25 μl out of a total of 200 μl of eluates were used for SDS-PAGE. WB was performed with antibody that recognizes total synapsin (Cell Signaling Technology, Inc., Danvers, MA) diluted 1:1000 and 110.6 Ab (anti-O-GlcNAc Ab, Covance Inc., Princeton, NJ) diluted 1:1000. In parallel, WB with 110.6 Ab pretreated for 30 min at 4 °C with 500 mM GlcNAc was performed as a control of Ab specificity; thus, the signal obtained after the pretreatment is nonspecific (28).

Expression Constructs—Rat synapsin Ia fused to N-terminal EGFP and C-terminal FLAG in pEGFP-C1 vector (Clontech) was kindly provided by Hung-Teh Kao, Brown University (29). To generate vectors for the expression of *O*-GlcNAc site-specific mutants of synapsin I, nucleic acid triplets encoding for serine or threonine residues that can be modified by *O*-GlcNAc were mutated to encode for alanines using QuikChange II site-directed mutagenesis kit (Stratagene, La Jolla, CA). See Table 1 for the list of the generated constructs and amino acid substitutions introduced.

Assessment of O-GlcNAc Levels on EGFP-Synapsin I—HEK293T cells were transfected with pEGFP-synapsin constructs using Lipofectamine 2000 (Invitrogen), according to the manufacturer's recommendations. 48 h after transfection, synapsin was immunoprecipitated using anti-FLAG M2 affinity gel (Sigma), according to the manufacturer's recommendations. While still on beads, the synapsin was transferred into the following buffer: 20 mM $Na_nH_nPO_4$ (pH 7.4), 12.5 mM $MgCl_2$, 500 μM UDP-GlcNAc, Complete protease inhibitor mixture tablets

(Roche Diagnostics); 5 μg of recombinant long isoform of nucleocytoplasmic OGT (ncOGT) was added, and the reaction was performed overnight at room temperature on a rotor. Then synapsin was eluted with 100 μg/ml FLAG peptide (Sigma), resolved on SDS-PAGE, and probed with 110.6 Ab diluted 1:1000 (Covance Inc, Princeton, NJ). ncOGT was expressed and purified as described previously (30). The expression vector was kindly provided by Dr. Suzanne Walker, Harvard University.

Dissociated Primary Hippocampal Cell Cultures—Pregnant E18 Holzman rats purchased from Harlan Laboratories, Indianapolis, IN, were euthanized using CO_2. Embryos were decapitated; hippocampi were removed, treated with 2.5% trypsin (Invitrogen) for 20 min, and serially triturated in the presence of 10 mg/ml DNase. The dissociated neurons were plated onto poly-D-lysine (Sigma)-coated german glass coverslips (Corning Glass) or homemade 35-mm video dishes for live imaging at a density of 200 cells/mm^2. Cells were plated in a plating medium consisting of DMEM and 10% horse serum (Invitrogen). After 2 h, the plating medium was replaced by culture medium that consisted of Neurobasal-A (Invitrogen), 2 mM glutamine, 2% B27 supplement (Invitrogen), 5% FBS (Gemini Bioproducts, West Sacramento, CA), and additional 25 mM glucose. Cultures were maintained at 37 °C in a 5% CO_2 humidified incubator. Every 4th day, one-third of the medium was replaced with fresh medium. Depending on the glial cell density, 5 μM cytosine arabinoside (Sigma) was added 3–5 days after plating to inhibit additional growth of glial cells. Cells were transfected with Lipofectamine 2000 (Invitrogen) after 5–7 days in culture and were subjected to live imaging on days 15–17.

Synapsin Targeting Factor—Primary hippocampal neurons were cotransfected with vectors expressing EGFP-synapsin (wild type or mutants) and DSRed2 (Clontech). Before imaging, media were substituted with perfusion solution to reduce background: 119 mM NaCl, 2.5 mM KCl, 2 mM $CaCl_2$, 2 mM $MgCl_2$, 5 mM HEPES (pH 7.4), 30 mM glucose (31). Localization of synapsin I to synapses was quantified by calculating the targeting factor (TF), a ratio of intensities of synaptic to axonal EGFP signal normalized to the same ratio calculated for DSRed2 (volume marker) minus 1 (29). Synapses were identified as puncta along neurites formed by EGFP. Intensities of axonal staining for EGFP-synapsin or DSRed2 were calculated as an average of median intensities of two areas circled in close proximity to a given synapse. Intensities were extracted using AxioVision4.8 software. TF values were distributed normally (Shapiro-Wilk normality test). Average values between biological replicates ±S.D. are reported. Pairwise comparisons between various mutants were performed using the two-tail *t* test, and Bonferroni corrected *p* values are reported for the six comparisons made.

SV Cluster Density—Primary hippocampal neurons were cotransfected with pEGFP-Syna1a or pEGFP-Syn1a_T87A, and synaptophysin subcloned into pmRFP1-N1 expression vector, which was kindly provided by Dr. Benjamin Odermatt, MRC Laboratory of Molecular Biology, United Kingdom (32). Before imaging, media were substituted with the perfusion solution. During the acquisition of images, the exposure time was kept constant for both red and green channels. Because a vast majority of mRFP puncta colocalized with EGFP puncta, SV clusters were defined as EGFP-mRFP-positive puncta. Median frequency of SV clusters was calculated along neurites for each biological replica ($n = 3$ pairs), and these values were compared between WT and T87A using a paired *t* test. Averages between biological replicates ±S.D. are reported. The acquired images were also used to calculate the total expression levels of Syn1a and Syn1a_T87A mutant. Borders of neurons expressing the indicated constructs were manually defined, and ratios of AFU for green channel per area were calculated. Average values ± S.E. were reported.

Quantitation of SV Pools by FM 4-64 Dye Staining and Analysis of Synapsin I Dispersion—Primary hippocampal neurons were transfected with pEGFP-Syna1a or pEGFP-Syna1a_T87A plasmids and later were loaded with FM 4-64 dye and imaged as described previously with some modifications (33). For quantification, synaptic boutons were loaded with FM 4-64, and the mean fluorescence in a region of interest determined by the EGFP signal was obtained for both channels during the time-lapse using ImageJ software. Because the intensity of FM 4-64 fluorescence across the population of boutons within the neuron was not distributed normally (Shapiro-Wilk normality test), the median value of FM 4-64 staining of boutons was calculated for each image/neuron. The total recycling pool of SVs at a synaptic bouton was calculated as the difference between FM 4-64 staining before the application of a 2-s stimulus at 20 Hz and the FM 4-64 staining at the end of imaging at the bouton. RRPSV was calculated as the difference between FM 4-64 staining before the application of a 2-s stimulus at 20 Hz and staining before the application of 180-s stimulus at 10 Hz and expressed as the % of total recycling pool of SVs. RPSV was calculated by subtraction of RRPSV from 100% (total recycling pool). For each neuron median RPSV was calculated. The averages between RPSV of neurons ± S.D. are reported to visualize difference between RPSV in WT and T87A synapsin I-expressing neurons. ANCOVA analysis was used to test differences in median size of RPSV between neurons expressing WT and T87A mutant synapsin I with expression of synaptic EGFP-synapsin as a covariate. Intensities of EGFP-synapsin fluorescence at synapses were extracted from the first time frame. To compare the speed of SVs released in neurons expressing WT or T87A mutant synapsin I in response to 10 Hz stimulation, parts of the destaining curves were fitted into single exponential decay, and half-lives of FM 4-64 fluorescence at synapses were calculated for each neuron (τ) and tested between the two groups by *t* test. Kinetic analysis of synapsin dispersion from synapses into axonal shafts after application of 10 Hz stimulation for 90 s was carried out as described previously (31). Dispersion curves ($-\Delta F/F_0$ *versus* time) were fitted into single exponential decay to obtain a half-life of synapsin at synapse (τ). $\Delta F = F_t - F_0$, where F indicates the mean intensity at a synapse and $F_t - F$ at a given time point; F_0 indicates the average F of six time points taken before the application of the stimulation. Average τ ±S.D. was reported.

Imaging Equipment—Imaging was performed on a Zeiss 200 M inverted microscope equipped with an Orca ER CCD camera (Hamamatsu). Zeiss pan-Neofluar 100× and 40× objectives with 1.3 and 0.17 numerical apertures, respectively, were used. FM 4-64 fluorescence was visualized by Wide Green filter set

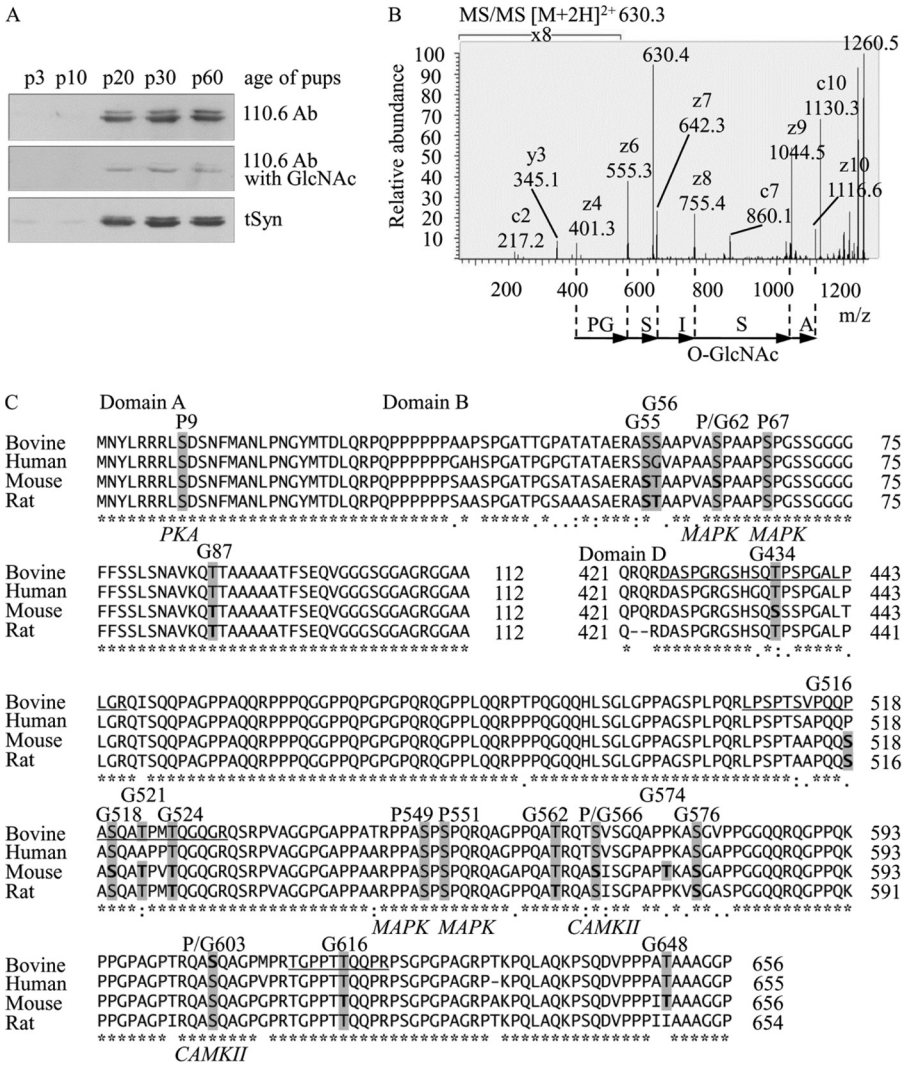

FIGURE 1. **Characterization of synapsin I *O*-GlcNAcylation.** *A,* WB analysis of synapsin I *O*-GlcNAcylation in rat hippocampi during development. Hippocampi dissected from rat pups of indicated ages were lysed, and synapsin I was pulled down from the lysates containing equal amount of protein. The samples were probed with antibodies that recognize total synapsin (*tSyn*) and *O*-GlcNAc (110.6). The two bands detected represent synapsin Ia and Ib. In the *middle panel,* 110.6 antibodies were pretreated with 500 mM GlcNAc to inhibit the recognition of *O*-GlcNAc by the antibody. Thus, only a nonspecific signal generated by 110.6Ab is detected. *p* stands for postnatal day. *B,* MS/MS electron transfer dissociation fragmentation spectra of a tryptic peptide QAS(*O*-GlcNAc)ISGPAPTK (starting position Gln-566) from bovine synapsin I identifies *O*-GlcNAc modification site Ser-568. *C,* amino acid sequence alignment of domains A, B, and D of synapsin I from indicated species with mapped or predicted *O*-GlcNAc and phosphorylation sites highlighted in *gray*. *P* or *G* above an amino acid symbol indicates whether it is a phosphorylation or *O*-GlcNAcylation site; numbering of sites is based on rat synapsin I sequence. Residues in *bold* were found to be *O*-GlcNAc-modified in this study on mouse and bovine synapsin I or by others on mouse and rat synapsin I. *Underlined* stretches of amino acids in bovine synapsin I indicate the peptides that were found to be modified by *O*-GlcNAc, but the site of the modification has not been assigned.

(Chroma Technology Corp., Bellows Falls, VT). Culture dish inserts from Warner Instruments (Hamden, CT) were used for field stimulation.

RESULTS

Synapsin I Is Modified by O-GlcNAc during Synaptogenesis—Synapsin I is modified by *O*-GlcNAc in the adult rat brain (22). Although synapsin I contributes to synaptogenesis and establishment of RPSV during development, its state of *O*-GlcNAcylation is not known during this time. In rat hippocampus, synaptogenesis happens postnatally. Synapsin I expression is induced during synaptogenesis and can be detected on the 3rd day after birth and plateaus at about 20 days after birth (34). To address if synapsin I *O*-GlcNAcylation might regulate synapsin I during synaptogenesis, we examined the temporal pattern of modification of synapsin I with *O*-GlcNAc during hippocampal synaptogenesis in rat. *O*-GlcNAc could be detected on synapsin I at postnatal day 20, when expression of synapsin I reaches maximum and remained at the same level during the rest of synaptogenesis up to day 60, indicating potential regulatory function of *O*-GlcNAc during this time (Fig. 1*A*).

Mapping O-GlcNAc Sites on Synapsin I—One goal of this study was to investigate site-specific roles of *O*-GlcNAc on synapsin I. Several *O*-GlcNAc sites have been previously mapped on purified rat synapsin I. The study utilized labeling of *O*-GlcNAcylated peptides with [^{3}H]galactose; however, several labeled peptides went unidentified, indicating potential unmapped *O*-GlcNAc sites (22). To comprehensively characterize *O*-GlcNAc sites and to address the conservation of *O*-GlcNAcylation patterns on synapsin I between species, we subjected tryptic peptides derived from purified mouse

or bovine synapsin I to LC-MS/MS. Three novel *O*-GlcNAc sites were mapped on synapsin I. Two of them are homologous to CaMKII phosphorylation sites Ser-566 and Ser-603 on rat synapsin I. Ser-568 (homologues to rat Ser-566) was the *O*-GlcNAc-modified residue within the mouse synapsin I peptide QASISGPAPTK (starting position Gln-566) (Fig. 1*B*). Ser-605 (homologous to rat Ser-603) was modified by *O*-GlcNAc within bovine synapsin I peptide QASQAGPMPR (starting position Gln-603) (supplemental Fig. 1). Another novel *O*-GlcNAc site mapped was Ser-436 in the mouse synapsin I peptide GSHSQSSSP-GALTLGR (starting position Gly-431). Mouse Ser-436 is homologous to bovine Thr-436. Peptide DASPGRGSHSQTPSP-GALPLGR (starting position Asp-425) from bovine synapsin containing Thr-436 was also *O*-GlcNAc-modified in our study (supplemental Fig. 1).

Thr-650, which is a known *O*-GlcNAc site on mouse synapsin Ia (11), was modified by *O*-GlcNAc here within peptide PAK-PQLAQKPSQDVPPPITAAAGGPPHPQLK (starting position Pro-632) belonging to mouse synapsin Ib. Ser-518 and Ser-576 were *O*-GlcNAc-modified on mouse synapsin I; these sites are homologous to known *O*-GlcNAc sites on rat synapsin I (22). Several *O*-GlcNAc sites that were previously mapped in proteomic studies were also detected by us, as for example on mouse synapsin I (supplemental Fig. 1) (9, 11). Of the now total 16 *O*-GlcNAc sites, 10 are conserved between human, bovine, mouse, and rat synapsin I (Fig. 1*C*). All identified *O*-GlcNAc sites mapped within domains B and D, the regulatory regions that are also heavily phosphorylated. Surprisingly, the level of conservation of *O*-GlcNAc sites (63%) is lower than the level of sequence identity of domains B (87%) and D (89%) of synapsin I between species.

Mutation of Domain B O-GlcNAc Sites to Alanine Increases Localization of Synapsin I to Synapses—At early stages of synaptogenesis, synapsin I is evenly distributed throughout axons in hippocampal cultures, but it increasingly localizes to synapses at later stages of synaptogenesis (35). Because we found that synapsin I is modified by *O*-GlcNAc during late stages of synaptogenesis, we sought to examine whether *O*-GlcNAcylation directly regulates localization of synapsin I to synapses. To investigate site-specific roles of *O*-GlcNAc on synapsin I in primary hippocampal neurons, we generated EGFP-fused mutants of synapsin I in which *O*-GlcNAc sites were converted to alanines, an amino acid that cannot be modified by *O*-GlcNAc. This approach has been previously used to study how site-specific phosphorylation regulates synapsin I function (29). Although phosphorylation at various sites was found to regulate activity-induced dispersion of synapsin I from synapses to axonal shafts (31), no evidence of regulation of synapsin I localization to synapses by post-translational modifications has been reported thus far (29).

Considering that multiple *O*-GlcNAc sites may work additively to regulate synapsin I, we generated mutants in which multiple *O*-GlcNAc sites were disrupted simultaneously, to maximize potential phenotypes of the mutants. We avoided mutation of *O*-GlcNAc sites that overlap with CaMKII or ERK phosphorylation sites, as interpretation of altered synapsin I function being due to *O*-GlcNAc would be confounded by the loss of phosphorylation at those sites as well. Thus, we generated rat synapsin Ia expression constructs with the following *O*-GlcNAc sites mutated: three *O*-GlcNAc sites within domain B (the expression construct is designated Syn1a_1–3); four, six, or all eight *O*-GlcNAc sites in domain D (designated Syn1a_5–8, Syn1a_5–10, and Syn1a_4–11, respectively); and all 11 *O*-GlcNAc sites (designated Syn1a_1–11) (Fig. 2*A* and Table 1).

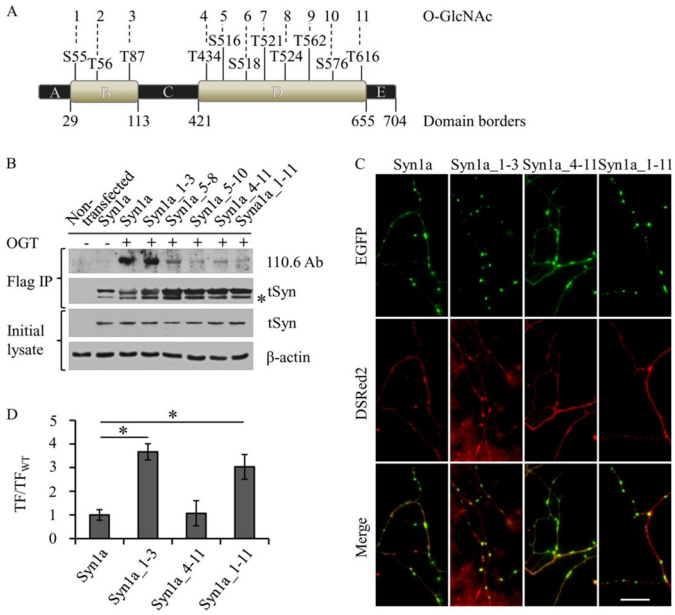

FIGURE 2. **Targeting of *O*-GlcNAc site-specific mutants of synapsin I to synapses.** *A,* schematic representation of the domain organization of synapsin I. Residues are numbered as in rat synapsin I. Numbers are assigned to *O*-GlcNAcylated residues that were mutated to alanines to generate various *O*-GlcNAc site-specific mutants of synapsin I. *B* and *C, numbers* that follow *Syn1a_* indicate *O*-GlcNAc sites that are mutated to alanines. *B,* WB analysis of *O*-GlcNAc levels on synapsin mutants. Wild type synapsin I and indicated *O*-GlcNAc site mutants were expressed in HEK293T cells, pulled down by FLAG-agarose, and *in vitro* modified by OGT. *O*-GlcNAc levels were analyzed by WB with 110.6 Ab. *, degradation product. *IP,* immunoprecipitation. *C,* localization of synapsin I *O*-GlcNAc site mutants in primary hippocampal neurons. On day 7 in culture, primary rat hippocampal neurons were cotransfected with plasmids expressing wild type or *O*-GlcNAc site mutants of EGFP-synapsin I and DsRed2 and were imaged on day 15. *Scale bar,* 10 μm. *D,* TF values were calculated from images like those in *C*. Each value represents an average TF of 3–6 biological replicates. For each biological replicate, TFs for 60–300 synapses were calculated. TF are normalized to TF of wild type synapsin. * indicates Bonferroni-corrected $p < 0.0001$.

Wild type synapsin I and the *O*-GlcNAc site-specific mutants were expressed at similar levels in HEK293T cells (Fig. 2*B*). Because the levels of *O*-GlcNAc modification, as detected by Western blotting with 110.6 Ab, were low on the exogenous wild type synapsin I, FLAG immunoprecipitations were performed, and wild type synapsin I and the mutants were modified by OGT *in vitro*. The *O*-GlcNAc site mutants displayed varying degrees of reduced *O*-GlcNAcylation, with a group of four residues, including Ser-516, Ser-518, Thr-521, and Thr-524, appearing to be responsible for most of *O*-GlcNAc signal on synapsin I, as detected by Western blotting with 110.6 antibody (Fig. 2*B*, Syn1a_5–8, *5th lane* compared with Syn1a, *3rd lane*). It is possible that 110.6 Western blotting of synapsin I mutants may not exactly reflect true relative changes in *O*-GlcNAc levels, as the 110.6 antibody may have varying affinities for *O*-GlcNAc sites depending on amino acid context and thus may not recognize all *O*-GlcNAc sites on synapsin I equally well. Next, EGFP-fused wild type and site-specific *O*-GlcNAc

mutants of synapsin I were coexpressed with DSReds2 in primary hippocampal neurons. In 15-day-old cultures, when synaptogenesis is complete, we analyzed localization of the EGFP-fused synapsin I using the "targeting factor" (TF) metric (29). TF is a ratio of synaptic to axonal EGFP signal normalized to the same value calculated for DSRed2, a soluble protein that evenly distributes in the neuronal cytoplasm and serves as a volumetric reporter. Quantitation of TF corrects the variations in EGFP-synapsin I expression between different neurons and the variations in EGFP-synapsin I signal due to changes in cell volume along axons. If TF equals zero, then the EGFP-tagged protein is distributed volumetrically along axons. TF above zero indicates synaptic targeting (29). Synapsin I with all *O*-GlcNAc sites mutated (Syn1a_1–11) displayed a 3.03 ± 0.2-fold increased TF compared with wild type synapsin I (Fig. 2, *C* and *D*; $p < 0.0001$), indicating that *O*-GlcNAc may be a negative regulator of synapsin I targeting to synapses. The observed targeting effect of the mutated *O*-GlcNAc sites is attributable to sites within domain B, because the Syn1a_1–3 mutant displayed a similar increase in synaptic targeting as the Syn1a_1–11 mutant and exhibited a 3.67 ± 0.17-fold increased TF compared with the TF of wild type synapsin I (Fig. 2, *C* and *D*; $p < 0.0001$). In contrast, localization of synapsin I with all *O*-GlcNAc sites in domain D mutated (Syn1a_4–11) was similar (1.07 ± 0.31-fold difference, nominal $p = 0.78$) to the localization of wild type synapsin I (Fig. 2, *C* and *D*). Since mutation of all *O*-GlcNAc sites from 4 to 11 does not contribute to the increased localization of Syn1a_1–11 to synapses. TFs were not quantified for the Syn1a_5–8 and Syn1a_5–10 mutants.

ERK Phosphorylation Sites Do Not Contribute to Altered Localization of Synapsin I Domain B O-GlcNAc Mutant—*O*-GlcNAc sites in domain B are proximal to two ERK phosphorylation sites (Fig. 1*C*). In some cases, *O*-GlcNAc has been shown to functionally compete with phosphorylation at nearby residues (36). We considered that loss of *O*-GlcNAc sites in domain B might result in increased phosphorylation at ERK phosphorylation sites and that this may contribute to increased synaptic localization of the synapsin I *O*-GlcNAc mutants. Synapsin I with *O*-GlcNAc sites in domain B mutated (S55A, T56A, and T87A) displayed increased phosphorylation at ERK sites Ser-62 and Ser-67 when expressed in HEK293T cells. In lysates where Syn1a_1–3 mutant was expressed, optical density of a band detected by an antibody that recognizes phosphorylated Ser-62 and Ser-67 was increased 15 ± 0.8 times compared with optical density of a band detected in lysates expressing wild type synapsin I (Fig. 3*A*, *2nd* and *4th lanes*), suggesting the possibility that *O*-GlcNAcylation interplays with phosphorylation at ERK phosphorylation sites in domain B of synapsin I in neurons. In primary hippocampal neurons, we analyzed how mutations that mimic or disrupt phosphorylation at synapsin I ERK phosphorylation sites influence the localization of synapsin I to synapses. Localization of wild type synapsin I was not affected by introduction of S62E and S67E substitutions that mimic constitutive phosphorylation (TF of the synapsin I mutant containing both substitutions increased 1.38 times ± 0.1 compared with wild type synapsin I but did not quite reach significance threshold even with nominal $p = 0.078$). Also, increased synaptic localization of synapsin I with *O*-GlcNAc sites in domain B mutated to alanines was not disrupted by introduction of S62A and S67A mutations that block phosphorylation at ERK sites, demonstrating that interplay with phosphorylation is not involved in the regulation of the targeting of synapsin I to synapses by *O*-GlcNAc (Fig. 3*B*).

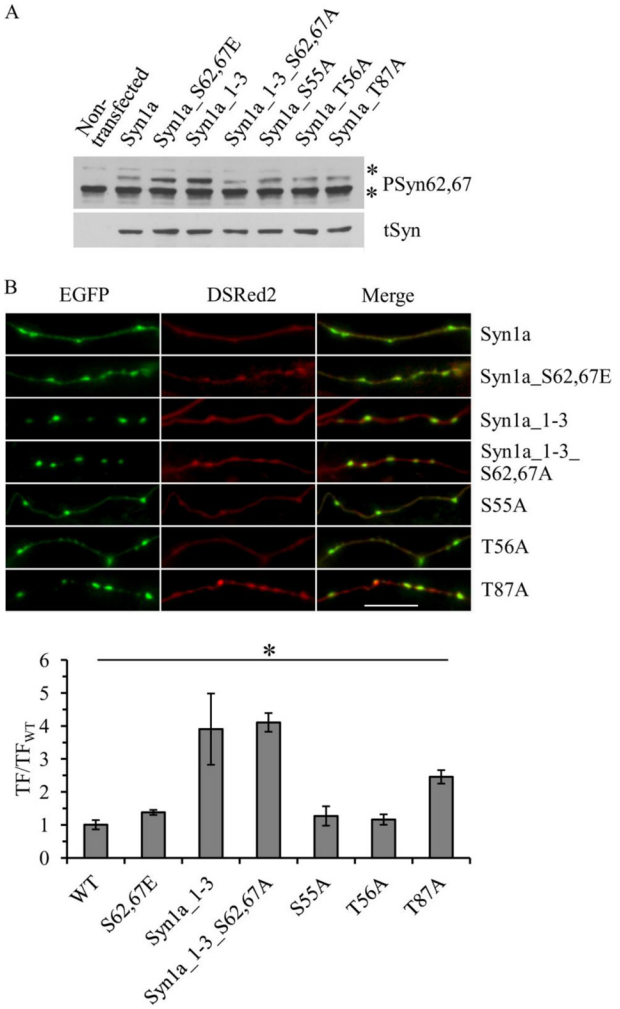

FIGURE 3. **Investigation of interplay between *O*-GlcNAc and ERK phosphorylation sites in domain B in regulation of synapsin I localization to synapses.** *Numbers* that follow *Syn1a_* indicate *O*-GlcNAc sites that are mutated to alanines, numbered as in Fig. 2*A*. In Syn1a_S62,67E mutant, serines 62 and 67 both were substituted to glutamate to mimic phosphorylation. In Syna1a_1–3_S62A,S67A mutant *O*-GlcNAc sites 1–3 as well as ERK phosphorylation sites Ser-62 and Ser-67 were mutated to alanines to create synapsin I that cannot be phosphorylated or modified by *O*-GlcNAc in domain B. *A,* HEK293T cells were transfected with wild type synapsin I or indicated mutants of synapsin I, lysed 48 h later, and subjected to WB with antibody that recognize total synapsin and synapsin phosphorylated at indicated ERK phosphorylation sites. *, nonspecific bands. *B,* localization of *O*-GlcNAc and ERK mutants of synapsin I in primary hippocampal neurons. *Upper panel,* neurons were cotransfected with plasmids expressing EGFP-tagged wild type or mutants of synapsin I, as indicated on the *right side of the panel* and DsRed2 on day 7 in culture, and were imaged on day 15. *Scale bar,* 10 μm. *Lower panel,* TFs were calculated from images like those on the *upper panel*. Each value represents an average TF of three biological replicates. For each biological replicate, TFs for at least 300 synapses were calculated. TFs are reported as relative to WT TF arbitrarily set at 1. * indicates Bonferroni-corrected $p < 0.05$.

O-GlcNAcylation Site Threonine 87 Regulates Synaptic Targeting of Synapsin I—To determine the contribution of individual *O*-GlcNAc sites in domain B to the regulation of synapsin I localization to synapses, we generated synapsin I mutants with single amino acid substitutions as follows: S55A, T56A, or

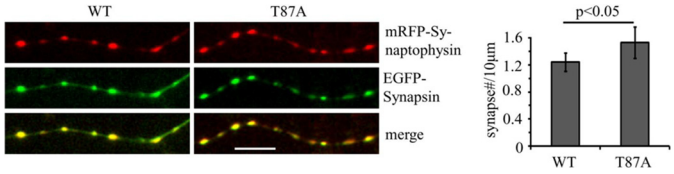

FIGURE 4. **SV cluster density in neurons expressing WT or T87A synapsin I.** Hippocampal neurons were cotransfected on day 5 with EGFP-Syn1a or EGFP-Syn1a_T87A and a plasmid for the expression of mRFP-synaptophysin. On day 15, live cultures were imaged. Synaptophysin served as a marker of SV clusters. *Scale bar,* 10 μm. *Right panel,* frequency of SV clusters along neurite is plotted. Because the vast majority of mRFP puncta colocalized with EGFP puncta, SV clusters were defined as EGFP-mRFP-positive puncta. Averages of three biological replicates were calculated. At least 800 synapses were counted for each biological replica.

T87A. Expression levels and phosphorylation at ERK phosphorylation sites of these mutants were similar to those of wild type synapsin I in 293T cells (Fig. 3*A*, *2nd* and *6th* to *8th lanes*). The localization of the T87A mutant was similar to the localization of synapsin I with all *O*-GlcNAc sites in domain B mutated, whereas S55A and T56A mutants localized similarly to wild type synapsin I (Fig. 3*B*). Thus, the mutation of the single *O*-GlcNAc modification site Thr-87 to alanine is responsible for increased localization of synapsin I to synapses. Synapsin I T87A mutant displayed no increased phosphorylation at ERK phosphorylation sites, further supporting the conclusion that regulation of synapsin I localization by *O*-GlcNAc is independent of ERK phosphorylation (Fig. 3*A*). Bright puncta formed by the synapsin I T87A mutant represented functional synaptic species of synapsin I, because they targeted to SV clusters, as defined by colocalization with an integral SV protein synaptophysin, and dispersed into axons upon high frequency stimulation (Figs. 4 and 5*E*, and more details in the text below). The expression levels of synapsin I T87A were similar to the expression levels of wild type synapsin I in primary hippocampal neurons: $AFU/area_{T87A} = 0.70 \pm 0.12$, $AFU/area_{WT} = 0.71 \pm 0.10$, $p = 0.96$, calculated from images as on Fig. 4 for 11 and 13 neurons, respectively (data not shown).

Expression of Synapsin I T87A Mutant Increases the Density of SV Clusters Along Axons—Synapsin I increasingly localizes to nascent synapses to support their development at a time when synapsin I becomes *O*-GlcNAc-modified. Synapsin I knock-out primary hippocampal neurons display delayed synaptogenic phenotypes, including reduced numbers of synapses (37). In contrast, overexpression of synapsin I leads to an increase in the number of synapses in primary hippocampal culture (38, 39). Therefore, we considered if the increased synaptic targeting of synapsin I T87A might correlate with an increase in the number of SV clusters along axons, especially as we observed higher numbers of EGFP-synapsin I puncta in neurons expressing the synapsin I T87A mutant compared with neurons expressing wild type synapsin I while quantifying synaptic targeting. To quantify this potential difference in SV clustering, we coexpressed wild type or T87A mutant EGFP-synapsin I with mRFP-synaptophysin in primary hippocampal neurons. Synaptophysin is an integral membrane protein of SVs and has been shown to localize to SV clusters when expressed exogenously (40). Puncta formed by wild type EGFP-synapsin I and the T87A *O*-GlcNAc site mutant colocalized with synaptophysin puncta, indicating targeting of both EGFP-synapsin I constructs to SV clusters (Fig. 4). We calculated the frequency of puncta positive for both EGFP-synapsin and synaptophysin-mRFP along neurites. SV cluster densities were 1.2 ± 0.14 and 1.5 ± 0.23 SV clusters/10 μm of neurite for wild type synapsin I and the T87A mutant, respectively, a significant difference at $p = 0.012$ (Fig. 4). The increased SV cluster density in T87A mutant was due to a higher number of SV clusters, as the length of axons was similar in neurons expressing wild type synapsin I or synapsin I T87A mutant (data not shown).

Expression of Synapsin I T87A Mutant Increases RPSV at the Expense of the RRPSV—Synapsin I contributes to the establishment of RPSV (12). The role of synapsin I in generating RPSV is critical in counteracting synaptic depression and thus in presynaptic plasticity (41). We considered that increased synaptic localization of synapsin I *O*-GlcNAc site mutant T87A may have functional consequences in determining the size of RPSV. To measure RPSV, we employed the dye FM 4-64, which emits fluorescence in lipid environments (*e.g.* when it is loaded in SVs (42)). The total recycling pool of SVs was loaded with FM 4-64 present in the media by intense depolarization (10 Hz during 2 min; Fig. 5*A*). During the depolarization, the total recycling pool was released, and FM 4-64 dye was taken up during subsequent endocytosis that replenishes the total recycling pool. RRPSV and RPSV, which collectively make up the total recycling pool, were differentially released by applying a specific stimulation protocol (Fig. 5*B*) (33). FM 4-64 fluorescence is lost when FM 4-64 is released from SVs back into the aqueous environment, allowing the measurement of SV pools (Fig. 5*B*) (33). The total recycling pools of SVs at synapses of neurons expressing wild type synapsin I or synapsin I with the T87A substitution were not statistically different (153 ± 22 $AFU_{FM\ 4\text{-}64}$ and 142 ± 23 $AFU_{FM\ 4\text{-}64}$, respectively, $p = 0.68$). However, synapses of neurons expressing the T87A mutant exhibited a 16% increase in RPSV (69.1 ± 4.3%) compared with RPSV of synapses expressing wild type synapsin I (59.5 ± 4.4%, $p = 0.001$) (Fig. 5*C*). These numbers probably underestimate the actual percent of SVs in the reserve pool, because bleaching contributed to some extent to FM 4-64 fluorescence loss at synapses during the depolarization. However, the difference between RPSV in neurons expressing wild type or T87A synapsin I is accurate because it remained constant during the course of FM 4-64 destaining and equals 9.6% of the SVs in the recycling pool (see the gap between the slopes of destaining curves for the neurons expressing wild type or T87A mutant synapsin I after 20 Hz stimulation, Fig. 5*B*). Thus, expression of T87A synapsin I mutant resulted in a shift in the distribution of SVs, as about 9.6% of the SVs in the recycling pool were observed to be in the RPSV instead of RRPSV, when compared with the distribution of SVs in neurons expressing wild type synapsin I.

Although increased synaptic localization of synapsin T87A corresponded to increased size of RPSVs, it was possible that mechanisms independent of increased synaptic localization contributed to the synapsin T87A phenotype of increased RPSVs. At individual synapses, there was no correlation between the amount of exogenous synapsin I present and the size of RPSV for either wild type or T87A mutant synapsin I (Pearson $r = 0.10$ for the wild type and $r = 0.23$ for T87A synapsin). However, expression levels of exogenous synapsin at

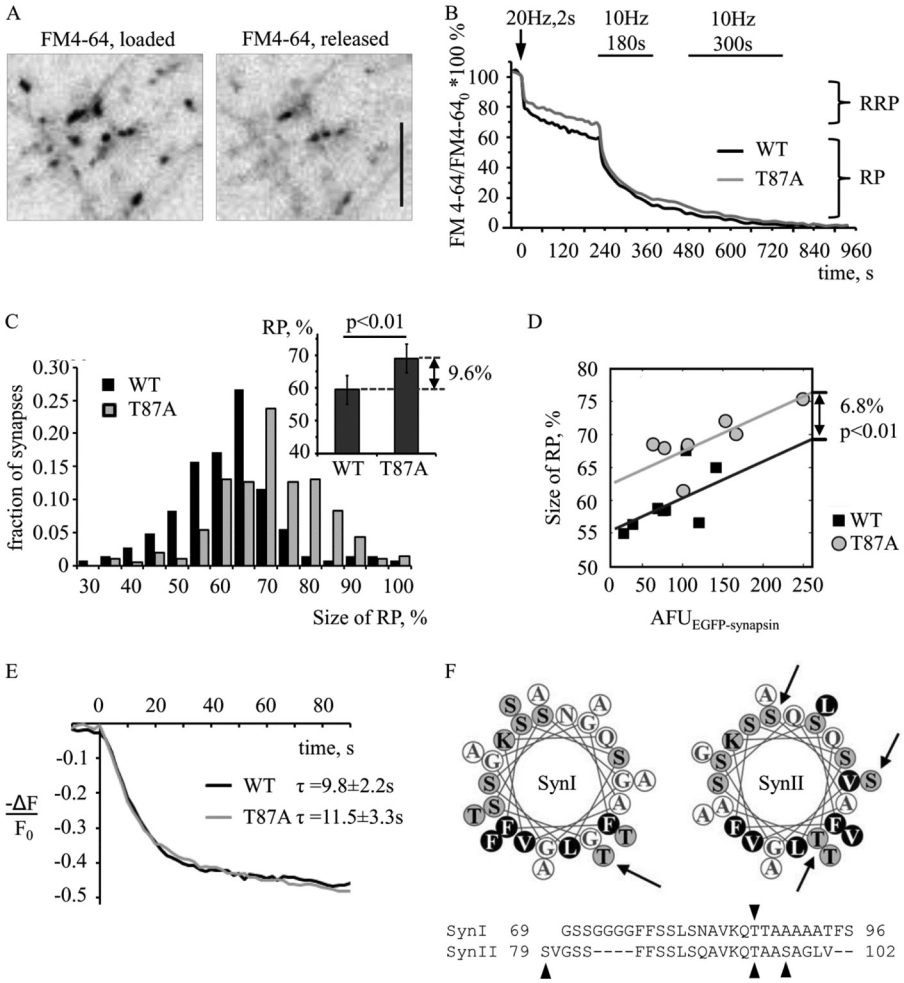

FIGURE 5. **Regulation of the RPSV by T87A synapsin I mutant.** *A–D,* analysis of functional pools of SVs. Primary hippocampal neurons were transfected with EGFP-Syn1a or EGFP-Syn1a_T87A on day 5 and stained with FM 4-64 dye and imaged on day 17. *A,* example of neurons loaded with FM 4-64 before (*left*) and after HFS (*right*). Images are inverted. Puncta that disappeared after HFS represent synapses where all SVs of the recycling pool were released. *Scale bar,* 10 μm. *B,* FM 4-64 destaining curves. Brief 20 Hz stimulation releases RRPSV (*RRP*) and two longer 10 Hz trains release RPSV (*RP*). Median values that were calculated from 147 (WT) and 207 (T87A) synapses from eight (WT) and seven (T87A) destaining experiments are plotted. *C,* frequency chart, fractions of synapses with RPSV of indicated sizes in neurons expressing WT and T87A synapsin I are plotted. *Inset*, average size of RPSV (% of total). Values are calculated from the destaining experiments, which are summarized in *B. D,* ANCOVA analysis of average RPSV size values between neurons expressing WT and T87A synapsin I mutant, with synaptic expression of EGFP-synapsin as a covariate. Average RPSV and EGFP values are from experiments summarized in *B. E,* synapsin I dispersion upon HFS. Neurons were transfected with EGFP-Syn1a or EGFP-Syn1a_T87A on day 7 and imaged on day 16. Dispersion of synapsin was triggered by 10 Hz stimulation for 90 s. Nine neurons (total 295 synapses) expressing WT synapsin and five neurons (total 387 synapses) expressing T87A synapsin were imaged. Average dispersion curves are shown. Average half-life of synapsin I at a synapse $\tau \pm$S.D. is reported. *F,* helical wheel projection of ALPS motif of synapsin I (on the *left*) and synapsin II (on the *right*). *Black circles* with *white letters* represent hydrophobic residues. *Gray circles* with *black residues* represent hydrophilic residues. Hydrophobic face of ALPS presumably faces SV and interacts with hydrophobic tails of lipid membrane. Hydrophilic face of ALPS faces cytosol and is proposed to interact with polar headgroups of lipid membrane of SVs. Alignment of ALPS motifs from rat synapsin I and II is shown *below*. *Arrows* and *arrowheads* indicate *O*-GlcNAc sites.

synapses averaged for single neurons positively correlated with the average size of RPSVs for that neuron (Pearson $r = 0.66$ for the wild type and $r = 0.72$ for T87A synapsin). To gain insight into the degree to which increased synapsin T87A synaptic localization contributed to observed increases in RPSV size, we performed an ANCOVA approach comparing the distribution of wild type and T87A synapsin I intensities at synapses in single neurons with increases in RPSV for those same neurons. The analysis revealed that a significant fraction of the RPSV increase in T87A-expressing neurons was independent of T87A-increased synaptic localization. As seen in Fig. 5*D*, in regions of distribution in which WT and T87A synaptic intensities overlap, there is still a clear increase in RPSV size for the T87A mutant. Put another way, the increase of RPSV in single neurons expressing T87A synapsin I was significant ($p = 0.004$) even when the same levels of synapsin wild type *versus* T87A synaptic intensity occurred in those single neurons. The expression of the T87A mutant, corrected for increased localization to synapses, resulted in an increase in RPSV of 6.82% over synapsin I wild type (Fig. 5*D*), suggesting that mechanisms beyond simply increasing the localization of synapsin I to synapses contribute to increased size of RPSV in neurons expressing the T87A synapsin I mutant. The speed of SV release after 10 Hz stimulation was similar in neurons expressing wild type or T87A synapsin I mutant: $\tau_{WT} = 37.9$ s and $\tau_{T87A} = 37.8$ s ($p = 0.44$, Fig. 5*B*).

Activity-induced Dispersion of Synapsin I into Axonal Shafts Is Not Affected by the Introduction of T87A Substitution—Upon HFS, synapsin I disperses into axonal shafts. Several phosphorylation sites regulate the speed of dispersion, which correlates

with the speed of SV exocytosis (20, 31). Because we did not observe differences in the speed of the release of SVs in wild type *versus* T87A synapsin I, activity-induced dispersion of synapsin I was likely not to be affected by the introduction of T87A substitution. Indeed, kinetic parameters of dispersion of wild type synapsin I and synapsin with T87A substitution were not statistically different, $\tau = 9.8 \pm 2.2$ and $\tau = 11.5 \pm 3.3$, respectively ($p = 0.28$) (Fig. 5*E*).

DISCUSSION

Our previous work linked *O*-GlcNAc to synaptic plasticity in hippocampus, as pharmacological elevation of *O*-GlcNAc in mouse brain facilitated long term potentiation involving a presynaptic mechanism (8). To begin to dissect how *O*-GlcNAc modulates presynaptic plasticity, in this study we tested the role of *O*-GlcNAc-modified residues on SV-associated protein synapsin I, which is known to play critical roles in presynaptic plasticity. The original description of synapsin I *O*-GlcNAcylation reported mapping of seven *O*-GlcNAc sites that clustered in proximity to phosphorylation sites known to contribute to synapsin I function (22). *O*-GlcNAc has in some cases been shown to functionally compete with phosphorylation at proximal sites. However, a lack of *in vitro* interplay between synapsin I *O*-GlcNAc and phosphorylation sites led the authors to conclude that synapsin *O*-GlcNAcylation likely has direct regulatory roles independent of influences on synapsin I phosphorylation (22).

We started with comprehensive characterization of *O*-GlcNAc sites on synapsin I and then used site-directed mutagenesis to selectively block synapsin I *O*-GlcNAcylation at specific sites and tested whether such mutations influence synapsin I biology linked to regulation of synaptic plasticity. We demonstrated that a single synapsin I *O*-GlcNAc site Thr-87 regulates synaptic localization of synapsin I, the density of SV clustering along axons, and the size of the RPSV, suggesting a possible role for synapsin I *O*-GlcNAcylation in regulation of presynaptic plasticity.

In previous studies, domain deletion analysis defined regions of synapsin I important for its synaptic localization and suggested association with SVs and dimerization with synapsin I or II as mechanisms involved in synaptic targeting of synapsin I (29). The *O*-GlcNAc site Thr-87 is located within a recently described ALPS motif. Disruption of the ALPS motif dramatically reduces the binding of synapsin I to SVs and decreases localization of synapsin I to synapses (43). Thus, the T87A substitution is likely to affect synaptic targeting of synapsin I by regulating the protein's association with SVs.

Structure-function relationships for several ALPS motifs, including the synapsin I ALPS motif have been previously investigated. This gives us an opportunity to discuss in more detail how T87A substitution may affect the ALPS motif on synapsin I. A typical ALPS motif is unstructured until it encounters lipid membrane (43–45). On highly curved membranes such as those of SVs, but not on more flat cell membranes, the ALPS motif folds into an α-helix. This behavior is dictated by its specific amino acid composition. When folded, the ALPS motif has defined hydrophobic and hydrophilic faces. The hydrophobic face of the helix interacts with fatty acid chains of lipids. It is composed of hydrophobic amino acids with relatively bulky side chains, which would not be able to intercalate between tightly packed lipids of flat membranes but can be inserted between loosely packed lipids of curved membranes, such as ones that form SVs. The hydrophilic face of the helix interacts with polar headgroups of lipids, which determine charge of a membrane. The hydrophilic face of ALPS motif is composed of hydrophilic but mostly uncharged amino acids. This renders the helix insensitive to the charge of a membrane and exacerbates sensitivity of the helix to membrane curvature. Thr-87 intercalates between hydrophobic residues on the hydrophobic side of the ALPS motif on synapsin I (Fig. 5*F*). The T87A substitution not only prevents *O*-GlcNAcylation in this region but also increases local hydrophobicity and thus may promote folding of the APLS motif on SVs, increasing affinity of synapsin I to SVs and perhaps contributing to the increased localization of synapsin I to synapses that we observe. We speculate that *O*-GlcNAcylation of Thr-87 has an opposite effect, because *O*-GlcNAc is bulky and hydrophilic and would probably interfere with folding of the ALPS motif and interaction of the ALPS motif with SV lipid membrane, thus decreasing affinity of synapsin I for SVs. Because OGT is believed to modify peptides in extended conformation, it is possible that OGT modifies the ALPS motif when it is unstructured. Function of *O*-GlcNAcylation in this case may be to decrease the binding of synapsin I to SVs or to protect the ALPS motif from misfolding while it is unstructured (46). We want to emphasize that although this model for regulation of synapsin I function by *O*-GlcNAc at Thr-87 is supported by our data, future studies in which the direct influence of Thr-87 *O*-GlcNAcylation on SV binding are required to confirm our model.

Based on secondary structure prediction, an ALPS motif is present in all isoforms of synapsin even though the amino acid composition of the motif is not conserved between the isoforms (44). Three *O*-GlcNAc sites have been recently mapped within a predicted ALPS motif of synapsin II (Fig. 5*F*) (11). Two of the synapsin II *O*-GlcNAc sites are within the hydrophobic face of the ALPS helix. The presynaptic scaffolding protein piccolo, involved in organization of SVs at the active zone, also contains predicted ALPS motifs within which *O*-GlcNAc sites have been mapped (10, 44). Thus, *O*-GlcNAc modification sites within ALPS motifs may be a regulatory mechanism influencing SV binding in proteins other than synapsin.

Expression of the synapsin I T87A mutant increased the size of RPSV, without affecting the total number of SVs. Two-thirds of the increase in RPSV appears to be independent of increased localization of the synapsin I T87A mutant to synapses. This observation may be explained when the current model showing how SVs are clustered together by synapsins is taken into account (47). It has been proposed that SVs within RPSV are bridged by homo- or heterodimers of synapsins I and II, with one molecule of synapsin being bound to one SV. It is possible that a fraction of synapsin dimers may be associated with only one SV, instead of two SVs, and thus does not participate in SV clustering. If the T87A substitution increases affinity of synapsin I to SVs, one can imagine that more synapsin dimers will be bound to two SVs, and thus more SVs will be clustered together to form RPSV. This would explain why the expression of synapsin I T87A mutant led to larger RPSV than would be pre-

dicted solely based on the increased localization of synapsin I T87A mutant to synapses.

Although our findings demonstrate that expression of the T87A mutant increases RPSV without affecting the total number of SVs, it has been reported that constitutive phosphorylation of synapsin I by ERK in domain B has the opposite effect, dramatically increasing RRPSV without affecting the total number of SVs. The functional outcome of such SV distribution is enhanced hippocampal synaptic plasticity, including increased CA1 long term potentiation and dramatically enhanced hippocampus-dependent learning (21). In contrast to the expression of the T87A mutant increasing RPSV, *O*-GlcNAcylation of synapsin I at Thr-87 may increase RRPSV and may recapitulate ERK phosphorylation effects on memory potentiation. Thus, by manipulating the folding of the ALPS motif on synapsin I (and II), or possibly its *O*-GlcNAcylation at Thr-87, it may be possible to modulate presynaptic plasticity, including disease states in which synapsin I function is compromised. For example, several mutations of synapsin I that lead to the decreased localization of synapsin I to synapses were identified in autism spectrum disorders and epilepsy, whereas major depressive disorder was linked to the reduced expression of synapsin I (15, 16, 48).

Although we do not know how modification of synapsin I by *O*-GlcNAc is regulated, we can propose a very preliminary model for the function of synapsin I *O*-GlcNAcylation in synaptic plasticity. OGT transferase and *O*-GlcNAcase are developmentally regulated in brain (2), and we show here that synapsin I is modified by *O*-GlcNAc during synaptogenesis. Our data indicate that *O*-GlcNAcylation of Thr-87 on synapsin I may regulate the localization of synapsin I at synapses, the number of synapses, and the distribution of SVs between functional pools. Thus, a physiological function of *O*-GlcNAc during synaptogenesis may be to establish a distribution of SVs between functional pools that is optimal for synaptic function. It is also possible that synapsin I *O*-GlcNAcylation may serve as a mechanism in synaptic plasticity by modulating the supply of SVs to the RRPSV during HFS. *O*-GlcNAc levels increase in response to neurotransmission (5, 6). Increased *O*-GlcNAcylation of synapsin I during neuronal activity may disrupt association of synapsin with SVs and contribute to regulation of SV trafficking from RPSV to RRPSV.

This and previous site-mapping studies demonstrated synapsin I *O*-GlcNAcylation at CaMKII and ERK phosphorylation sites (11). The possible interplay between *O*-GlcNAc and CaMKII and ERK phosphorylation at the same sites may add additional levels of complexity to synapsin regulation by *O*-GlcNAc, as well as possible regulation of OGT and *O*-GlcNAcase activities during synaptogenesis or in mature neurons.

Acknowledgments—We thank Dr. Olimpia Meucci and Dr. Gordon Lutz from Drexel University College of Medicine for sharing protocols and help with the equipment. We also thank Dr. Benjamin Odermatt, MRC Laboratory of Molecular Biology (United Kingdom) for pmRFP1-N1-synaptophysin plasmid; Dr. S. Walker, Harvard University, for ncOGT expression construct; and Dr. Hung-Teh Kao from Brown University for pEGFP-synapsinIa vector.

REFERENCES

1. Cole, R. N., and Hart, G. W. (2001) Cytosolic *O*-glycosylation is abundant in nerve terminals. *J. Neurochem.* **79,** 1080–1089
2. Liu, Y., Li, X., Yu, Y., Shi, J., Liang, Z., Run, X., Li, Y., Dai, C. L., Grundke-Iqbal, I., Iqbal, K., Liu, F., and Gong, C. X. (2012) Developmental regulation of protein *O*-GlcNAcylation, *O*-GlcNAc transferase, and *O*-GlcNAcase in mammalian brain. *PLoS One* **7,** e43724
3. Fülöp, N., Feng, W., Xing, D., He, K., Not, L. G., Brocks, C. A., Marchase, R. B., Miller, A. P., and Chatham, J. C. (2008) Aging leads to increased levels of protein *O*-linked *N*-acetylglucosamine in heart, aorta, brain, and skeletal muscle in Brown-Norway rats. *Biogerontology* **9,** 139–151
4. Cheung, W. D., and Hart, G. W. (2008) AMP-activated protein kinase and p38 MAPK activate *O*-GlcNAcylation of neuronal proteins during glucose deprivation. *J. Biol. Chem.* **283,** 13009–13020
5. Khidekel, N., Ficarro, S. B., Clark, P. M., Bryan, M. C., Swaney, D. L., Rexach, J. E., Sun, Y. E., Coon, J. J., Peters, E. C., and Hsieh-Wilson, L. C. (2007) Probing the dynamics of *O*-GlcNAc glycosylation in the brain using quantitative proteomics. *Nat. Chem. Biol.* **3,** 339–348
6. Rexach, J. E., Clark, P. M., Mason, D. E., Neve, R. L., Peters, E. C., and Hsieh-Wilson, L. C. (2012) Dynamic *O*-GlcNAc modification regulates CREB-mediated gene expression and memory formation. *Nat. Chem. Biol.* **8,** 253–261
7. Song, M., Kim, H. S., Park, J. M., Kim, S. H., Kim, I. H., Ryu, S. H., and Suh, P. G. (2008) *O*-GlcNAc transferase is activated by CaMKIV-dependent phosphorylation under potassium chloride-induced depolarization in NG-108-15 cells. *Cell. Signal.* **20,** 94–104
8. Tallent, M. K., Varghis, N., Skorobogatko, Y., Hernandez-Cuebas, L., Whelan, K., Vocadlo, D. J., and Vosseller, K. (2009) *In vivo* modulation of *O*-GlcNAc levels regulates hippocampal synaptic plasticity through interplay with phosphorylation. *J. Biol. Chem.* **284,** 174–181
9. Vosseller, K., Trinidad, J. C., Chalkley, R. J., Specht, C. G., Thalhammer, A., Lynn, A. J., Snedecor, J. O., Guan, S., Medzihradszky, K. F., Maltby, D. A., Schoepfer, R., and Burlingame, A. L. (2006) *O*-Linked *N*-acetylglucosamine proteomics of postsynaptic density preparations using lectin weak affinity chromatography and mass spectrometry. *Mol. Cell. Proteomics* **5,** 923–934
10. Trinidad, J. C., Barkan, D. T., Gulledge, B. F., Thalhammer, A., Sali, A., Schoepfer, R., and Burlingame, A. L. (2012) Global identification and characterization of both *O*-GlcNAcylation and phosphorylation at the murine synapse. *Mol. Cell. Proteomics* **11,** 215–229
11. Alfaro, J. F., Gong, C. X., Monroe, M. E., Aldrich, J. T., Clauss, T. R., Purvine, S. O., Wang, Z., Camp, D. G., 2nd, Shabanowitz, J., Stanley, P., Hart, G. W., Hunt, D. F., Yang, F., and Smith, R. D. (2012) Tandem mass spectrometry identifies many mouse brain *O*-GlcNAcylated proteins, including EGF domain-specific *O*-GlcNAc transferase targets. *Proc. Natl. Acad. Sci. U.S.A.* **109,** 7280–7285
12. Bykhovskaia, M. (2011) Synapsin regulation of vesicle organization and functional pools. *Semin. Cell Dev. Biol.* **22,** 387–392
13. Rizzoli, S. O., and Betz, W. J. (2005) Synaptic vesicle pools. *Nat. Rev. Neurosci.* **6,** 57–69
14. Corradi, A., Zanardi, A., Giacomini, C., Onofri, F., Valtorta, F., Zoli, M., and Benfenati, F. (2008) Synapsin-I- and synapsin-II-null mice display an increased age-dependent cognitive impairment. *J. Cell Sci.* **121,** 3042–3051
15. Garcia, C. C., Blair, H. J., Seager, M., Coulthard, A., Tennant, S., Buddles, M., Curtis, A., and Goodship, J. A. (2004) Identification of a mutation in synapsin I, a synaptic vesicle protein, in a family with epilepsy. *J. Med. Genet.* **41,** 183–186
16. Fassio, A., Patry, L., Congia, S., Onofri, F., Piton, A., Gauthier, J., Pozzi, D., Messa, M., Defranchi, E., Fadda, M., Corradi, A., Baldelli, P., Lapointe, L., St-Onge, J., Meloche, C., Mottron, L., Valtorta, F., Khoa Nguyen, D., Rouleau, G. A., Benfenati, F., and Cossette, P. (2011) SYN1 loss-of-function mutations in autism and partial epilepsy cause impaired synaptic function. *Hum. Mol. Genet.* **20,** 2297–2307
17. Cesca, F., Baldelli, P., Valtorta, F., and Benfenati, F. (2010) The synapsins: Key actors of synapse function and plasticity. *Prog. Neurobiol.* **91,** 313–348
18. Hosaka, M., Hammer, R. E., and Südhof, T. C. (1999) A phospho-switch

controls the dynamic association of synapsins with synaptic vesicles. *Neuron* **24,** 377–387
19. Stefani, G., Onofri, F., Valtorta, F., Vaccaro, P., Greengard, P., and Benfenati, F. (1997) Kinetic analysis of the phosphorylation-dependent interactions of synapsin I with rat brain synaptic vesicles. *J. Physiol.* **504**, 501–515
20. Chi, P., Greengard, P., and Ryan, T. A. (2003) Synaptic vesicle mobilization is regulated by distinct synapsin I phosphorylation pathways at different frequencies. *Neuron* **38,** 69–78
21. Kushner, S. A., Elgersma, Y., Murphy, G. G., Jaarsma, D., van Woerden, G. M., Hojjati, M. R., Cui, Y., LeBoutillier, J. C., Marrone, D. F., Choi, E. S., De Zeeuw, C. I., Petit, T. L., Pozzo-Miller, L., and Silva, A. J. (2005) Modulation of presynaptic plasticity and learning by the H-ras/extracellular signal-regulated kinase/synapsin I signaling pathway. *J. Neurosci.* **25,** 9721–9734
22. Cole, R. N., and Hart, G. W. (1999) Glycosylation sites flank phosphorylation sites on synapsin I: *O*-linked *N*-acetylglucosamine residues are localized within domains mediating synapsin I interactions. *J. Neurochem.* **73,** 418–428
23. Bähler, M., and Greengard, P. (1987) Synapsin I bundles F-actin in a phosphorylation-dependent manner. *Nature* **326,** 704–707
24. Schröder, E., Jönsson, T., and Poole, L. (2003) Hydroxyapatite chromatography: altering the phosphate-dependent elution profile of protein as a function of pH. *Anal. Biochem.* **313,** 176–178
25. Chalkley, R. J., Thalhammer, A., Schoepfer, R., and Burlingame, A. L. (2009) Identification of protein *O*-GlcNAcylation sites using electron transfer dissociation mass spectrometry on native peptides. *Proc. Natl. Acad. Sci. U.S.A.* **106,** 8894–8899
26. Skorobogatko, Y. V., Deuso, J., Adolf-Bryfogle, J., Adolf-Bergfoyle, J., Nowak, M. G., Gong, Y., Lippa, C. F., and Vosseller, K. (2011) Human Alzheimer's disease synaptic *O*-GlcNAc site mapping and iTRAQ expression proteomics with ion trap mass spectrometry. *Amino Acids* **40,** 765–779
27. Schiebler, W., Jahn, R., Doucet, J. P., Rothlein, J., and Greengard, P. (1986) Characterization of synapsin I binding to small synaptic vesicles. *J. Biol. Chem.* **261,** 8383–8390
28. Zachara, N. E. (2009) Detecting the "O-GlcNAc-ome"; detection, purification, and analysis of *O*-GlcNAc modified proteins. *Methods Mol. Biol.* **534,** 251–279
29. Gitler, D., Xu, Y., Kao, H. T., Lin, D., Lim, S., Feng, J., Greengard, P., and Augustine, G. J. (2004) Molecular determinants of synapsin targeting to presynaptic terminals. *J. Neurosci.* **24,** 3711–3720
30. Gross, B. J., Kraybill, B. C., and Walker, S. (2005) Discovery of *O*-GlcNAc transferase inhibitors. *J. Am. Chem. Soc.* **127,** 14588–14589
31. Chi, P., Greengard, P., and Ryan, T. A. (2001) Synapsin dispersion and reclustering during synaptic activity. *Nat. Neurosci.* **4,** 1187–1193
32. Granseth, B., Odermatt, B., Royle, S. J., and Lagnado, L. (2006) Clathrin-mediated endocytosis is the dominant mechanism of vesicle retrieval at hippocampal synapses. *Neuron* **51,** 773–786
33. Gitler, D., Cheng, Q., Greengard, P., and Augustine, G. J. (2008) Synapsin IIa controls the reserve pool of glutamatergic synaptic vesicles. *J. Neurosci.* **28,** 10835–10843
34. Petersen, K., Olesen, O. F., and Mikkelsen, J. D. (1999) Developmental expression of α-synuclein in rat hippocampus and cerebral cortex. *Neuroscience* **91,** 651–659
35. Fletcher, T. L., Cameron, P., De Camilli, P., and Banker, G. (1991) The distribution of synapsin I and synaptophysin in hippocampal neurons developing in culture. *J. Neurosci.* **11,** 1617–1626
36. Hu, P., Shimoji, S., and Hart, G. W. (2010) Site-specific interplay between *O*-GlcNAcylation and phosphorylation in cellular regulation. *FEBS Lett.* **584,** 2526–2538
37. Chin, L. S., Li, L., Ferreira, A., Kosik, K. S., and Greengard, P. (1995) Impairment of axonal development and of synaptogenesis in hippocampal neurons of synapsin I-deficient mice. *Proc. Natl. Acad. Sci. U.S.A.* **92,** 9230–9234
38. Zhong, Z. G., Noda, M., Takahashi, H., and Higashida, H. (1999) Overexpression of rat synapsins in NG108-15 neuronal cells enhances functional synapse formation with myotubes. *Neurosci. Lett.* **260,** 93–96
39. Perlini, L. E., Botti, F., Fornasiero, E. F., Giannandrea, M., Bonanomi, D., Amendola, M., Naldini, L., Benfenati, F., and Valtorta, F. (2011) Effects of phosphorylation and neuronal activity on the control of synapse formation by synapsin I. *J. Cell Sci.* **124,** 3643–3653
40. Bamji, S. X., Shimazu, K., Kimes, N., Huelsken, J., Birchmeier, W., Lu, B., and Reichardt, L. F. (2003) Role of β-catenin in synaptic vesicle localization and presynaptic assembly. *Neuron* **40,** 719–731
41. Rosahl, T. W., Spillane, D., Missler, M., Herz, J., Selig, D. K., Wolff, J. R., Hammer, R. E., Malenka, R. C., and Südhof, T. C. (1995) Essential functions of synapsins I and II in synaptic vesicle regulation. *Nature* **375,** 488–493
42. Newton, J., and Murthy, V. (2006) Measuring exocytosis in neurons using FM labeling. *J. Vis. Exp.* **1,** 117
43. Krabben, L., Fassio, A., Bhatia, V. K., Pechstein, A., Onofri, F., Fadda, M., Messa, M., Rao, Y., Shupliakov, O., Stamou, D., Benfenati, F., and Haucke, V. (2011) Synapsin I senses membrane curvature by an amphipathic lipid packing sensor motif. *J. Neurosci.* **31,** 18149–18154
44. Drin, G., Casella, J. F., Gautier, R., Boehmer, T., Schwartz, T. U., and Antonny, B. (2007) A general amphipathic α-helical motif for sensing membrane curvature. *Nat. Struct. Mol. Biol.* **14,** 138–146
45. Antonny, B. (2011) Mechanisms of membrane curvature sensing. *Annu. Rev. Biochem.* **80,** 101–123
46. Lazarus, M. B., Nam, Y., Jiang, J., Sliz, P., and Walker, S. (2011) Structure of human *O*-GlcNAc transferase and its complex with a peptide substrate. *Nature* **469,** 564–567
47. Shupliakov, O., Haucke, V., and Pechstein, A. (2011) How synapsin I may cluster synaptic vesicles. *Semin. Cell Dev. Biol.* **22,** 393–399
48. Kang, H. J., Voleti, B., Hajszan, T., Rajkowska, G., Stockmeier, C. A., Licznerski, P., Lepack, A., Majik, M. S., Jeong, L. S., Banasr, M., Son, H., and Duman, R. S. (2012) Decreased expression of synapse-related genes and loss of synapses in major depressive disorder. *Nat. Med.* **18,** 1413–1417